The influence of organic complexation on Ni isotopic fractionation and Ni recycling in the upper soil layers

Isabella O. Zelano, C. Cloquet, F. Fraysse, Shuofei Dong, Noemie Janot, Guillaume Echevarria, Emmanuelle Montargès-Pelletier

https://doi.org/10.1016/j.chemgeo.2018.02.023

The influence of organic complexation on Ni isotopic fractionation and Ni recycling in the upper soil layers

Isabella O. Zelano[1,2,], Christophe Cloquet[1], Fabrice Fraysse[2], Shuofei Dong[1], Noémie Janot[2], Guillaume Echevarria[3], Emanuelle Montargès-Pelletier[2]*

[1] CRPG, UMR 7358, CNRS-Université de Lorraine, 54501, Vandœuvre-lès-Nancy, France

[2] LIEC, UMR 7360, CNRS-Université de Lorraine, 54500, Vandœuvre-lès-Nancy, France

[3] LSE, UMR 1120 INRA Université de Lorraine, 54500 Vandœuvre-lès-Nancy, France

* corresponding author e-mail : zelano@crpg.cnrs-nancy.fr

ABSTRACT. The quantification of Ni isotopic fractionation induced by Ni binding to organic acids is a preliminary step to better constrain the mechanisms determining Ni isotopic fingerprint observed in surface soils, waters and plants, as well as the contribution of metal recycling during plant litter degradation. In this study, Ni isotopic fraction induced by reaction with small organic acids, e.g. citric and oxalic acids, and with soil purified humic acids (PHA) was investigated at different Ni-L ratio and pH conditions. The Donnan Membrane Technique was used to separate Ni bound to organic ligands from the free metal. Obtained results highlighted that Ni binding with carboxylic groups produces, in the adopted experimental conditions, a $\Delta^{60}Ni_{bond\text{-}free} < 0.2‰$. This value is not high enough to justify neither metal fractionation previously observed between soil and hyperaccumulators, nor the fractionation between different plant parts, e.g. roots and leaves. In parallel, leaf degradation experiments of two hyperaccumulating plants, where Ni is mainly present as Ni-citrate, were performed to simulate litter decomposition and to highlight the contribution of plants on Ni isotopic composition in surface soils and waters. In the case of the hyperaccumulator Alyssum murale, the degradation process did not induce any observable fractionation. On the contrary, during Rinorea bengalensis degradation experiment, a fractionation between Ni leached out in the first 10 days and between 10 and 30 days was observed ($\Delta^{60}Ni_{10–30day} = 0.20 \pm 0.05‰$). The observed fractionation evidenced a heterogeneous distribution of Ni within the leaves, and/or distinct chemical bonding to the leaf cells, and finally suggested the influence of the chemical bonding on Ni isotopic signature. Although a precise quantification of plant contribution on Ni isotopic signature in surface soils and waters is still not reached, our results produced important progress to elucidate the role of organic matter in regulating Ni isotopic fingerprint in surface layers.

KEYWORDS
Ni; Isotopic fractionation; Complexation; Organic matter; Hyperaccumulating plants

https://doi.org/10.1016/j.chemgeo.2018.02.023

1. Introduction

Being a biologically active trace metal, Ni is thought to have had a crucial role in the early Earth (Willaims and Frausto da Silva, 2003; Domagal-Goldman et al., 2008) and during the last decade nickel isotopes have attracted increasing interest as a new tool to investigate biogeochemical processes at Earth's surface. The biogeochemical processes controlling Ni isotopic fractionation in surface layers are, however, not yet well understood and require further investigations. In the Earth's crust, Ni is mostly present under the +2 oxidation state (Ni^{2+}) (Fujii et al., 2014) and undergoes redox reactions mainly through anthropogenic processes (Ni metallurgy) (Ratié et al., 2015a). Thus, it is assumed that redox processes cannot be responsible for the different Ni isotopic signatures observed in terrestrial samples as opposed to other metals, such as Fe, Cu and Cr (Wiederhold, 2015). Although the current literature data about Ni isotopic compositions are still quite limited, they highlight an important dispersion of δ^{60}Ni values among the different studied Earth's surface samples (Ratié et al., 2015a). Indeed, a relatively small Ni variation in isotopic composition of terrestrial samples has been measured, including eruptive rocks (basalts) and continental sediments, with an average $\delta^{60}Ni$ value of +0.15‰ ± 0.24‰ (Cameron et al., 2009). In contrast with those abiotic materials, an isotopic fingerprint between −0.44 ± 0.20‰ and −1.46 ± 0.08‰ was observed for Ni-containing methanogen bacteria in respect to the culture medium, suggesting a high potential of Ni stable isotopes as biomarkers of methanogenesis on the early Earth (Cameron et al., 2009; Cameron et al., 2007; Cameron et al., 2012). Studying for the first time the isotopic composition of dissolved Ni in ocean and river waters, Cameron and Vance (2014) pointed out a nickel isotopic mass balance incoherence. On one hand, they reported an average $\delta^{60}Ni$ value of 1.44‰ ± 0.15‰ in a homogeneous set of seawater, consistent with the range of the $\delta^{60}Ni$ values measured for organic-rich marine sediments (0.2‰ to 2.5‰) (Porter et al., 2014) and for the ferromanganese crust (0.9‰ to 2.5‰, with an average of $\delta^{60}Ni$ = 1.6 ± 0.8‰) (Gall et al., 2013), both representing the principal output of Ni from the oceans (Gall et al., 2013). On the other hand, dissolved Ni in river waters, supposed to be a considerable Ni ocean input, presented highly variable isotopic compositions, with δ^{60}Ni ranging between 0.29‰ and 1.34‰. Thus the δ^{60}Ni values measured for continental waters are not high enough to explain δ^{60}Ni values in seawater, even though they are up to 1‰ heavier than the reported values for continental silicate rocks (Cameron and Vance, 2014), suggesting a major influence of weathering processes on Ni isotopic fractionation. Few results have been reported about Ni isotope fractionation due to weathering (Gall et al., 2013; Ratié et al., 2015b). For instance, Ratié et al. (2015b) investigated the effects of weathering on lateritic profile of ultramafic sites, showing that formation of Ni-bearing clays and Fe-oxides induced a depletion of Ni heavy isotopes in the solid phases as well as their export in the dissolved phase, $\Delta^{60}Ni_{soil\text{-}bedrock}$ up to −0.47‰. These results are consistent with the $\delta^{60}Ni$ values measured in the exchangeable pool of an ultramafic soil, the labile pool, which were higher than those of the corresponding bulk sample (average $\Delta^{60}Ni_{exch\text{-}tot}$ = 0.29‰ (Ratié et al., 2015b)). Those data were also in good agreement with Ni sorption/precipitation experiments onto ferrihydrite, where a preferential adsorption of light isotopes onto the solid phase was observed, $\Delta^{60/58}Ni_{dissolved\text{-}sorbed}$ = + 0.35 ± 0.10‰ (Wasylenki et al., 2015; Wang and Wasylenki, 2017).

Up to now, no data is available concerning Ni isotopic fractionation after complexation with soil organic matter. Nevertheless, metals present a high affinity for humic substances, which are a dominant phase influencing metal bioavailability. Moreover, even though it is widely assumed that biogeochemical cycle of metals is influenced by biotic processes, only few data have been published on the role of living organisms on Ni isotopic fractionation (Deng et al., 2014; Estrade et al., 2015). A fundamental example is hyperaccumulators, that are plants characterized by a unique capability to accumulate extremely high concentration of metals in their biomass (Van der Ent and Mulligan, 2015). Most of those plants are nickel hyperaccumulators, with a nominal threshold con-

centration fixed at 1000 μg g^{-1} foliar Ni (Reeves, 2003). Replenishment of available Ni pools in soils through the biogeochemical recycling represents, therefore, a considerable contribution to Ni global cycle. This contribution is even more important in the context of ultramafic areas, which are among the most important Ni continental reservoirs, and where hyperaccumulators mainly grow. Hyperaccumulators found in ultramafic complexes of Mediterranean Region are mainly in the genus of *Alyssum* (Brassicaceae), while several different families are present in tropical ultramafic outcrops, e.g. *Rinorea bengalensis* (Violacee), *Phyllantus securinegioides* (Phyllanthaceae), etc. (Van der Ent and Mulligan, 2015). Despite the increasing attention dedicated to hyperaccumulating plants, suitable for soil remediation and agromining activity (Van der Ent et al., 2015), the ecological reasons for nickel hyperaccumulation are still not well understood (Van der Ent and Mulligan, 2015). The role of those plants in nickel cycle is, however, crucial as they represent, together with the precipitation of secondary minerals, the major sink for metals. Moreover, the potential contribution of vegetation on Ni isotopic composition in the upper soil horizon and its influence on Ni exportation towards aqueous compartments has been advanced (Estrade et al., 2015). However, the discrimination of stable isotopes of Ni within plants through accumulation processes has just been unraveled with a preliminary study so far (Deng et al., 2014; Estrade et al., 2015). Similarly, it is recognized that plant litter degradation is one of the main source of dissolved major and trace elements in rivers (Fraysse et al., 2010; Pokrovsky et al., 2005), but no data has been published concerning the study of Ni isotopic fractionation potentially occurring during litter degradation process. A complete investigation of Ni cycle, including plant uptake and plant recycling, deserves, therefore, a greater attention. Deng et al. (2014) performed experiments on plants grown in hydroponic conditions and showed a preferential uptake of light Ni isotopes by plants. In another study, plants naturally grown on ultramafic systems were investigated reporting a whole-plant isotopic composition heavier than the soil, with $\Delta^{60}Ni_{\text{whole plant-soil}}$ up to 0.40‰, but lighter than the bioavailable pool, $\Delta^{60}Ni_{\text{DTPA-rhizosoil}}$ up to 0.89‰ (Estrade et al., 2015). This supports the hypothesis that the bioavailable Ni in soil presents a heavy isotopic signature compare to the total soil, and that plants probably take up the lighter fraction of isotopes from this heavy pool.

A considerable number of processes are known to involve Ni binding to organic molecules, such as mobilization and uptake of nutrients by plants and microorganisms, detoxification processes by plants, microbial proliferation and dissolution of soil minerals (Marschner and Marschner, 2012; Jones, 1998). Among all the organic ligands produced by biological entities and slow degradation of biological material in soils, waters and sediments, the principal group consists of molecules bearing carboxylate functional groups. Those organic ligands commonly occur as low-molecular-weight molecules, such as acetate, malate, citrate, oxalate, and as macromolecules, such as humic substances (Strathmann and Myneni, 2004; Thurman, 1985). The isotopic composition of Ni in plants can be, then, strongly correlated to the potential isotopic fractionation induced by complexation with organic ligands involved in uptake mechanisms by root cells (Deng et al., 2014), in translocation and storage mechanisms in aerial parts of the plant, as well as by complexation with organic ligands present in soil solutions. The quantification of potential Ni isotopic fractionation when reacting with organic ligands is, therefore, necessary to elucidate the role of organic matter in the biogeochemical cycle of Ni.

In the present study, we aimed to determine the extent of Ni isotopic fractionation due to interaction with Purified Humic Acid (PHA), used as a proxy surrogate for reactive soil organic matter, and with oxalic and citric acids, both being representative of low-molecular weight organic molecules, involved in Ni plant uptake and storage processes (Jones, 1998). To this purpose, the Donnan Membrane Technique (DMT) (Temminghoff et al., 2000) was used to separate free Ni (Ni^{2+}) from the Ni bound to organic ligands (Ni-L) after complexation reaction. The DMT system consists of a donor and an acceptor solution divided by a negatively charged membrane, only permeable to free metal. The DMT has often been used to study

metal interaction with organic and inorganic ligands, both in laboratory and field applications (Kalis et al., 2006). However, the combination of this technique and the investigation of metal isotopic fractionation as a consequence of metal-ligand interaction has only been applied to Zn (Jouvin et al., 2009) and Cu (Ryan et al., 2014) so far. In this work, the combined effects of pH and degree of complexation between Ni and organic ligands on metal isotopic fractionation were investigated. This approach allows unravelling the influence of Ni interaction with organic molecules on Ni isotopic composition, which is still missing for a correct interpretation of Ni biogeochemical cycling. Moreover, in a second part of the work, the role of vegetation recycling in the upper soil layers was studied simulating, in controlled conditions, leaf degradation of two hyperaccumulators: *Alyssum murale*, a small shrub from temperate area, and a tropical young tree of *Rinorea bengalensis*, potentially growing up to 25 m high. This experiment aims to furnish new information necessary to introduce biological processes contribution in Ni isotopic cycle. Up to now, indeed, nothing is known, qualitatively and quantitatively, about how plant accumulation and release processes can modify Ni isotopic signature. To this purpose, Ni concentration and isotopic signature in leached solutions were monitored as a function of time, and results were interpreted on the basis of Ni speciation in plant leaves previously reported in literature, and on isotopic signature of Ni^{2+} and Ni-L, determined with DMT system.

2. Materials and methods

All reagents were prepared using ultrapure water (18.2 MΩ cm^{-1}). Nitric (HNO_3) and hydrochloric (HCl) acids were of supra-pure grade. The Humic Acid (PHA) was extracted from peat soils collected in São Paulo State, Brazil, purified following the International Humic Substances Society (IHSS) procedure. Element standard solutions were supplied by TechLab (1000 μg mL^{-1}, in a 2 to 5% HNO_3). Nickel solution for DMT experiments was diluted and a working solution at pH = 5 was prepared for avoiding a drastic decrease of pH in HA solution.

2.1. Nickel speciation with Donnan Membrane Technique

Experiments were conducted by using the DMT to quantify a potential Ni isotopic fractionation resulting from metal interaction with small organic acids and with PHA. The procedure applied in this study was modified from the one described by Pan et al. (2015).

2.1.1. System set-up

The system is made of two solutions, a donor and an acceptor, separated by a cation exchange membrane. The donor side consisted of 250 mL of $Ni(NO_3)_2$ aqueous solution, containing $Ca(NO_3)_2$ as supporting electrolyte, and the selected organic ligand. The acceptor solution was inside a cylindrical poly(methyl methacrylate) (PMMA) cell filled with 10 mL of the same $Ca(NO_3)_2$ electrolyte solution, and directly immersed in the donor solution from which it was separated by two cation-exchange membranes (supplied by VWR). The membranes are negatively charged and only the free hydrated cation can permeate through it, allowing the equilibration of free hydrated ion Ni^{2+} between the two sides. The small volume of the acceptor side was chosen to reduce the equilibration time and the quantity of Ni passing from donor to acceptor, avoiding, therefore, any alteration of the equilibrium in the donor solution (Ryan et al., 2014). Since the equilibration time for divalent cations was previously estimated to be between 48 and 72 h (Temminghoff et al., 2000; Weng et al., 2001), an equilibration time of 72 h was adopted.

As a preliminary step, membranes were washed to remove any undesired cations from their surface. Membranes were, therefore, immersed for at least 30 min in the following solutions: 1 M ethylene-diaminetetraacetic acid (EDTA), 18 MΩ water, 0.1 M HNO_3, 18 MΩ water. A 1 M $Ca(NO_3)_2$ was also used to saturate membrane surfaces. Each step was repeated twice. Finally, membranes were conditioned with 2 mM $Ca(NO_3)_2$ solution. PMMA vessels were washed twice in 5% HNO_3 and rinsed with 18 MΩ water.

2.1.2. Preliminary tests for isotopic fractionation due to Ni adsorption onto membranes

As already reported in literature for Zn and Cu (Jouvin et al., 2009; Ryan et al., 2014), the DMT can be a useful tool to study isotopic fractionation of a metal due to the interaction with a ligand. This is possible only if no isotopic fractionation is induced by metal sorption onto the membranes. Preliminary experiments were, therefore, conducted to verify this assumption by immersing three membranes in 100 mL of 5 μM $Ni(NO_3)_2$ aqueous solution and three membranes in 100 mL 5 μM Ni in 2 mM $Ca(NO_3)_2$. After three days of interaction, membranes were recovered and washed three times with 20 mL of 1 M HNO_3, and Ni concentration and isotopic composition were measured in the final and initial solutions. In a second step, the complete DMT device was tested in absence of ligand in the donor side, made of 600 mL 5 μM $Ni(NO_3)_2$ solution in 2 mM $Ca(NO_3)_2$. After three days of interaction, acceptor and donor solutions were recovered, all membranes were washed as described above and Ni concentration and isotopic composition were measured in all solutions. No significant difference was observed between the $\delta^{60}Ni$ of the membrane wash and the original Ni solution, neither in the preliminary tests, nor between donor, acceptor and membrane washing solutions (Table S1 of Supplemental Information (SI)).

2.1.3. Ni binding to organic ligands and Ni speciation calculation

Experimental conditions were chosen on the base of speciation calculations performed using Visual MinteQ v. 3.0 code released by USEPA.

In all experiments, Ni concentration was 50 μM in 2 mM $Ca(NO_3)_2$. The pH value was adjusted with NaOH or HNO_3 in the donor solution. For each different ligand concentration at least two replicates were performed. The ligand concentrations were 0.01 mM (pH = 5–7) for oxalic acid, 0.01 mM (pH = 5–7) and 0.1 mM (pH = 7) for citric acid. For both 0.01 mM oxalic and citric acid, about 10% of Ni was expected to be complexed, while for 0.1 mM citric acid, > 65% was predicted. No experiment was conducted with 0.1 mM oxalic acid because of the oversaturation of Ca-oxalate complexes. In all investigated cases, the formation of a monodentate complex between Ni and ligand was predicted. Solutions of PHA were prepared at 40, 80 and 110 mg/L (pH = 7), and 30%, 50% and 60% of metal was expected to be complexed. Nickel interaction with PHA was predicted using the NICA-Donnan model, in which the NICA equation discriminates metal specifically bound to the humic acid through its carboxylic and phenolic groups, and the Donnan equation quantifies the metal bound through electrostatic interaction (Kinniburgh et al., 1996; Benedetti et al., 1995). The proton-binding parameters (b, $\log K_{H,1}$, $\log K_{H,2}$, $n_{H,1}$, $n_{H,2}$, $Q_{max,1}$ and $Q_{max,2}$) values used were the ones determined specifically for the material used in this work. Heterogeneity parameters p_1 and p_2 and ion-binding parameters (Ca- and Ni-) values used were the generic ones for humic acids (Milne et al., 2003).

2.2. Plant leaf degradation experiment

Degradation experiments were performed on leaves of the hyperaccumulator plants *Alyssum murale*, supplied by ENSAIA-LSE, Université de Lorraine, cultivated on the ultramafic area in Pojskë, Pogradec, South-East of Albania (Bani et al., 2007), and on leaves of *Rinorea Bengalensis*, collected in the ultramafic area of Sabah, Borneo, Malaysia. Experiments were conducted on leaves dried in oven at moderate temperature (40 °C), to avoid drastic transformations of plant tissue and to reduce artificial effects on metal release. *A. Murale* leaf samples were delivered cut in pieces of about 0.5 cm, deriving from different plants. On the contrary, *R. bengalensis* leaves derived from one young plant of about 1.5 m high and leaves were cut in pieces of about 2–4 cm. 80 mg of dry sample were put in a 50kD Spectra/Por® 7 dialysis membrane, filled with 10 mL of $5 \cdot 10^{-4}$ M $NaNO_3$ solution. Dialysis membranes were then set in a 250 mL Teflon beaker filled up with $5 \cdot 10^{-4}$ M $NaNO_3$ solution and the beaker solution was gently agitated with a magnetic stirrer, to enhance solution exchange through the dialysis membrane. The reactors were plunged in a thermostated water-bath at 25 ± 0.2°C. The input solutions were injected in the reactors by a peristaltic pump with a flow rate of 0.5 mL min^{-1}. Experiments were

performed with $5 \cdot 10^{-5}$ M NaN_3 as a biocide on *R. Bengalensis* to inhibit the microbial respiratory activity, and without and with the biocide on *A. Murale*, to highlight the potential kinetic and isotopic differences induced by microbial activity. Measuring major and minor element concentrations in the output solutions as a function of time monitored the reaction progress. For each sampling time, between 20 mL and 40 mL of solution were collected and pH and conductivity were measured before acidification with few µL of concentrated HNO_3.

2.3. Metal concentration

Metal concentrations in DMT solutions and in leaching solutions of degradation experiments were determined with X-Series Inductively Coupled Plasma Mass Spectrometer (ICP-MS Quadrupole) supplied by Thermo Fisher Scientific. Leaves of *A. Murale* and *R. Bengalensis* and DMT solutions containing PHA (preliminary dried), were acid digested with 3 mL of aqua regia for 24 h at 140°C, and recovered with 0.3 M HNO_3.

2.4. Ni isotopic measurements

Before Ni isotopic determination, samples were subjected to a purification procedure necessary to remove sample matrix. The applied protocol was the one fully detailed by Estrade et al. (2015), based on the works of Cameron et al. (2009) and Gueguen et al. (2013). Briefly, a known amount of sample solution was evaporated (acid digested when needed) to get the 1–2 µg of Ni. Samples were then dissolved again in 3M HNO_3 and mixed with a double-spike solution containing an equal amount of ^{61}Ni and ^{62}Ni isotopes, in order to have a spike/sample ratio of 1.15. After over-night equilibration, samples were dried down and re-dissolved in 1 mL 6M HCl before purification. Two successive chromatographic separations were performed, using the anion-exchange resin AG1-X8 and a Ni-specific resin, supplied by Triskem Inc., France, which complexes Ni^{2+} with dimethylglyoxime between pH 8 and 9. A procedural blank was prepared and measured in each analytical session and estimated to contain between 5 and 15 ng of Ni. Nickel isotopic signature in all samples was measured by MC-ICP-MS (Neptune plus, Thermo Scientific) equipped with an Apex HF desolvation introduction system. All samples and standards were diluted to 200 µg L^{-1} in 0.3 M HNO_3 and measurements were performed in medium resolution. The use of a double Ni spike allowed the correction of the instrumental mass bias.

Once measured, Ni isotopic composition in samples was normalized using standard bracketing method relative to NIST-986 and reported as $\delta^{60}Ni$:

$$\delta^{60}\mathrm{Ni} = \left(\frac{^{60/58}\mathrm{Ni}_{sample}}{^{60/58}\mathrm{Ni}_{NIST\,986}} - 1\right) \times 1000\,(\mathrm{in}\,‰) \quad (1)$$

The long term analytical reproducibility was assessed by measuring the used Ni stock solution all along the experiments, obtaining an average value of $\delta^{60}Ni = -0.11 \pm 0.05‰$ (2SD, n = 25).

The external reproducibility was monitored by measuring ten times the reference material BHVO-2, obtaining $\delta^{60}Ni = 0.05 \pm 0.04‰$ (2SD), in agreement with published values. When 2SD value associated to measurements was lower than long term analytical reproducibility, the value of 0.05‰ value was used.

2.5. System isotopic mass balance and calculation of Ni-L isotopic signature

The isotopic mass balance of the system was assessed by summing the contribution of all DMT system compartments, as reported in Eq. 2:

$$x_I \cdot \delta^{60}\mathrm{Ni}_I = \frac{x_A \cdot \delta^{60}\mathrm{Ni}_A + x_D \cdot \delta^{60}\mathrm{Ni}_D + x_M \cdot \delta^{60}\mathrm{Ni}_M}{x_{tot-meas}}$$

where x_I is the initial amount (µmol) of Ni in the donor solution, x_A, x_D *and* x_M are respectively the amounts (µmol) measured in acceptor, donor solutions and membrane rinsing solution, and $x_{tot\text{-}meas}$ is the amount of Ni (µmol) recovered in the entire DMT system ($x_A+x_D+x_M$). $\delta^{60}Ni_I$, $\delta^{60}Ni_A$, $\delta^{60}Ni_D$ and $\delta^{60}Ni_M$ are the isotopic compositions of Ni in the initial solution, and in acceptor, donor and membrane rinsing solutions after equilibration, respectively.

Despite membranes were previously conditioned as described above to limit Ni^{2+} adsorption onto the negative charged sites, up to 25% of the initial amount of Ni was adsorbed onto the mem-

branes (Table 1). This contribution must, therefore, be taken into account to calculate the isotopic fractionation of Ni due to its complexation with organic ligands, i.e. $\delta^{60}Ni\text{-}L$. For this purpose, the Eqs. 3–4, already used by Jouvin et al. (2009), were adopted:

$$x_{Dtot} = \frac{x_{Mb}}{2} + x_{Dmeas} \quad (3)$$

where x_{Dtot} is the total amount of Ni on the donor side (μmol), x_{Dmeas}, is the amount of Ni (μmol) measured in the donor side, and x_{Mb}, the amount of Ni (μmol) adsorbed onto the membranes, assumed to be half of Ni in the membrane leach, (x_{Mb}/2). Eqs. 4 and 5 were, therefore, used to calculate $\delta^{60}Ni\text{-}L$:

$$\begin{aligned} x_{Dtot}\cdot\delta^{60}\mathrm{Ni}_D = {} & ¿ \\ & (x_{Mb}/2)\cdot\delta^{60}\mathrm{Ni}_{Mb} + ¿ \\ & x_{Dmeas}\,F_{\mathrm{Ni2+}}\cdot\delta^{60}\mathrm{Ni}^{2+} + ¿ \\ & x_{Dmeas}(1-F_{\mathrm{Ni2+}})\cdot\delta^{60}\mathrm{Ni\text{-}L} \end{aligned} \quad (4)$$

$$\delta^{60}\mathrm{Ni\text{-}L} = ¿ \frac{[x_{Dtot}\cdot\delta^{60}\mathrm{Ni}_D - (x_{Mb}/2)\cdot\delta^{60}\mathrm{Ni}_{Mb} - x_{Dmeas}F_{\mathrm{Ni2+}}\cdot\delta^{60}\mathrm{Ni}^{2+}]}{[x_{Dmeas}(1-F_{\mathrm{Ni2+}})]}$$

where $\delta^{60}Ni^{2+}$ is the isotopic composition of Ni^{2+} measured in the acceptor. F_{Ni2+} is the fraction of the free hydrated Ni^{2+} in the donor side, estimated from $[Ni^{2+}]$ measured in the acceptor and corrected for the effect of the ionic strengths (Temminghoff et al., 2000):

$$\frac{[\mathrm{Ni}^{2+}]_D}{[\mathrm{Ni}^{2+}]_A} = \frac{[\mathrm{Ca}^{2+}]_D}{[\mathrm{Ca}^{2+}]_A} \quad (6)$$

where $[Ni^{2+}]_A$, $[Ca^{2+}]_A$ and $[Ca^{2+}]_D$ are the concentration of Ni and Ca measured in the acceptor and donor sides, and $[Ni^{2+}]_D$ is the unknown concentration of free Ni in the donor. The isotopic fractionation between Ni bound to the organic ligand and the free hydrated Ni^{2+}, $\Delta^{60}Ni_{bound\text{-}free}$, was calculated as the difference between the calculated isotopic signature of organo-Ni complexes ($\delta^{60}Ni\text{-}L$) and the measured isotopic signature of free hydrated Ni^{2+} ($\delta^{60}Ni^{2+}$), as follows:

$$\Delta^{60}\mathrm{Ni}_{\mathrm{bound-free}} = (\delta^{60}Ni\text{-}L) - (\delta^{60}Ni^{2+}) \quad (7)$$

All experiments were conducted at least in duplicate and measured three times each. The external reproducibility is reported as 2σ, (n = 3). The average values X of experimental duplicates x_m are reported as:

$$X = x_m \pm \delta_{xm} \quad (8)$$

where:

$$\delta_{xm} = \frac{\sum_{x=1}^{N}\sigma_x}{\sqrt{N}} \quad (9)$$

The standard deviation σ associated to $\Delta^{60}Ni$ takes into account the error propagation, calculated as:

$$y = a+b, \sigma y = \sqrt{(\sigma a)^2 + (\sigma b)^2} \quad (10)$$

3. Results and Discussion

3.1. Nickel-PHA interaction

Nickel complexation with PHA ranged between 30% and 57% (Table 1), which was in good agreement with Ni complexation rate predicted by NICA-Donnan model. The 110 mg_{PHA} L^{-1} was the highest ligand concentration that could have been used without observing coagulation of macromolecules, provoked or enhanced by the high Ca concentration in solution.

As it can be observed on Fig. 1, no trend can be identified as a function of Ni complexation rate. The measured $\delta^{60}Ni_A$ and $\delta^{60}Ni_D$ (Table 2) both present not distinguishable values, within uncertainties, from the isotopic composition of the Ni starting solution ($\delta^{60}Ni_I$ = −0.11 ± 0.05, Table S1) and, consequently, δ^{60}Ni-PHA could not be calculated.

In those experimental conditions, NICA-Donnan model predicted Ni interaction with PHA mainly through carboxylic sites binding (Table SI2). At pH = 7, the model predicts that contribution of phenolic sites remains under 1.5%, the electrostatic binding to PHA represents between 2% and 2.5% of total Ni and Ni inorganic complexes were negligible. Jouvin et al. (2009) repor-

Table 1. *Nickel-ligand complexation rate, Ni concentration in Acceptor and Donor sides, and in Membrane leach of DMT system, after reaction with organic acids (citric and oxalic) and with humic acids (HA) at different pH and ligand concentration.*

Initial Ni in donor solution, µmol; 12.5	n.	%Ni-L	[Ni], µM			Ni %			µmol				Recovery %	µmol
			Acceptor	Donor	Membrane	Acceptor	Donor	Membrane	Acceptor	Donor	Membrane	Tot Ni		Free Ni in donor
Citric acid 0.01 mM	1	18.9	28.3	37.9	52.5	2.3	76.5	21.2	0.3	9.5	2.6	12.4	99.0	7.1
pH 7	2	10.5	29.7	34.7	51.9	2.4	70.1	21.0	0.3	8.7	2.6	11.6	92.6	7.4
	3	11.2	29.5	34.8	52.1	2.4	70.3	21.1	0.3	8.7	2.6	11.6	92.9	7.4
Citric acid 0.01 mM	1	19.1	28.1	37.8	53.0	2.3	76.3	21.4	0.3	9.4	2.6	12.4	99.0	7.0
pH 5	2	16.2	29.2	37.2	51.0	2.4	75.2	20.6	0.3	9.3	2.5	12.1	97.2	7.3
	3	16.0	29.6	37.6	51.5	2.4	76.0	20.8	0.3	9.4	2.6	12.3	98.2	7.4
Citric acid 0.1 mM	1	69.8	9.4	42.8	21.4	0.8	86.5	10.4	0.1	10.7	1.3	12.1	96.7	2.3
pH 7	2	67.2	10.0	43.1	25.7	0.8	87.0	12.5	0.1	10.8	1.5	12.4	99.3	2.5
Oxalic acid 0.01 mM	1	18.8	30.2	39.6	41.8	2.4	80.0	20.3	0.3	9.9	2.5	12.7	101	7.6
pH 7	2	19.5	29.8	39.5	43.0	2.4	79.9	20.8	0.3	9.9	2.6	12.8	102	7.4
	3	19.5	30.1	39.9	40.4	2.4	80.5	19.6	0.3	10.0	2.4	12.7	101	7.5
Oxalic acid 0.01 mM	1	17.6	31.7	40.5	38.7	2.6	81.8	18.7	0.3	10.1	2.3	12.8	102	7.9
pH 5	2	19.3	30.9	40.5	37.8	2.5	81.8	18.3	0.3	10.1	2.3	12.7	101	7.7
	3	16.7	31.4	39.6	37.7	2.5	80.0	18.3	0.3	9.9	2.3	12.5	99.8	7.8
HA 40 mg/L	1	30.3	22.8	39.1	44.9	1.8	76.1	21.8	0.2	9.4	2.7	12.3	98.8	5.7
	2	30.1	23.6	39.9	42.7	1.9	77.8	20.7	0.2	9.6	2.6	12.4	99.4	5.9
	3	29.7	24.3	40.8	43.0	2.0	79.4	20.9	0.2	9.8	2.6	12.7	101	6.1
HA 80 mg/L	1	47.9	16.9	43.1	36.9	1.4	83.4	17.9	0.2	10.3	2.2	12.7	101	4.2
	2	47.5	17.1	42.7	36.0	1.4	82.7	17.5	0.2	10.2	2.2	12.6	100	4.3
	3	46.9	16.7	41.3	36.1	1.3	80.1	17.5	0.2	9.9	2.2	12.2	98.0	4.2
HA 110 mg/L	1	55.8	21.9	43.9	31.4	1.8	88.7	13.9	0.2	11.0	1.7	12.9	103	5.5
	2	58.5	20.1	42.4	31.9	1.6	85.7	14.2	0.2	10.6	1.8	12.6	100	5.0

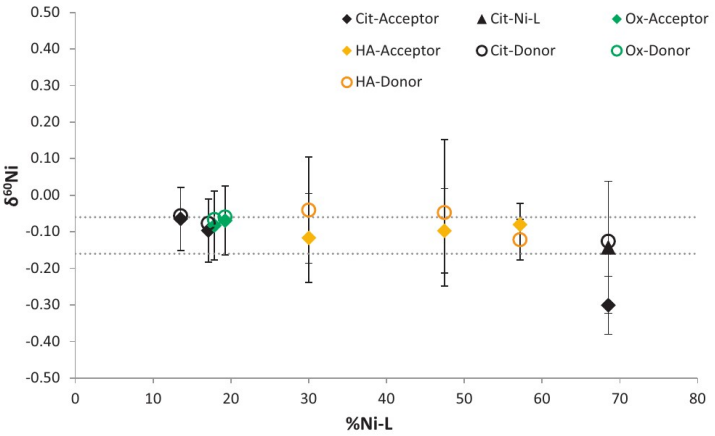

Fig. 1*. Ni isotopic composition measured in acceptor (diamonds) and donor sides (empty circles), for citric acid (black), oxalic acid (green) and PHA (yellow), and calculated $\delta^{60}Ni$ for Ni-Citrate (triangles), as a function of Ni complexation degree (%Ni-L). Grey dot lines represent 2σ uncertainty interval of the Ni starting solution, $\delta^{60}Ni_I = -0.11 \pm 0.05$.*

ted that no isotopic fractionation was measurable for Zn below pH = 6, but they calculated $\Delta^{66}Zn_{PHA\text{-}freeZn} = +0.24 \pm 0.06‰$ at pH = 7, when the contribution of phenolic groups became more relevant (Jouvin et al., 2009). Authors, therefore, attributed the observed isotopic fractionation to Zn interaction with phenolic groups, which have a higher binding constant ($\log K_{Zn\text{-}phenolic} = 2.39$) than carboxylic sites ($\log K_{Zn\text{-}carboxylic} = 0.11$). This hypothesis was also supported by the measured bond length ZneO for carboxylate (2.00 Å) and phenolate groups (1.91 Å), indicating a stronger interaction with the latter (Karlsson and Skyllberg, 2007). In the case of Cu interacting with insolubilized HA (IHA), Wilcke (2010) reported $\Delta^{65}Cu_{IHA\text{-}solution} = +0.26 \pm 0.11‰$ but no effect of pH was observed. Moreover, they modeled $\Delta^{65}Cu_{phenolic/carboxylic\text{-}solution} = +0.27‰$ without any difference between the two types of sites even if Cu presents a larger difference between the two constants than Zn ($\log K_{Cu\text{-}phenolic} = 6.85$. $\log K_{Cu\text{-}carboxylic} = 2.23$) (Milne et al., 2003). Similarly, Ryan et al., (2014) reported $\Delta^{60}Cu_{complex\text{-}free} = +0.14 \pm 0.11‰$ between

Cu and Suwannee River Fulvic Acid, without any variation as a function of pH. They underlined, however, that Cu is known to have a higher affinity for humics than several other metals (Pandey et al., 2000) and they suggested that pH should only slightly influence Cu isotopic fractionation due to the strong binding constants over a wide pH range. However, a strong correlation between the stability constants of Cu complexes with natural and synthetic ligands and the magnitude of the isotopic fractionation was reported (Ryan et al., 2014). In the hypothesis that complexation rate constants are correlated to the magnitude of the isotopic fractionation, the absence or the small Ni isotopic fractionation observed in this study is consistent with the low generic values reported for phenolic and carboxylic groups (Milne et al., 2003), $\log K_{\text{Ni-phenolic}} = -0.26$ and $\log K_{\text{Ni-carboxylic}} = 1.0$.

3.2. Ni-citric/oxalic acid interaction

Nickel concentration and isotopic signature measured in DMT system compartments are reported in Tables 1–2 and represented on Fig. 1.

Both at pH 5 and 7, in presence of 0.01 mM citric and oxalic acid, the percentage of Ni-com-

Table 2. *Nickel isotopic composition, δ^{60}Ni, and relative external reproducibility (2σ, n = 3) in the Acceptor, Donor and Membrane leach, after reaction with organic acids (citric and oxalic) and with purified humic acids (PHA). The error associated with average values of experimental replicates was calculated as reported in Eqs. 8–9. The δ^{60}Ni-L and Δ^{60}Ni values are calculated according to Eqs. 4, 5–7; the propagation error was calculated according to Eq. 10.*

δ^{60}Ni initial solution − 0.11‰	n	%Ni-L	Acceptor δ^{60}Ni	2σ	Donor δ^{60}Ni	2σ	Membrane δ^{60}Ni	2σ	Ni isotopic mass balance δ^{60}Ni			Ni-L δ^{60}Ni			Δ^{60}Ni		
Citric acid 0.01 mM pH 7	1	18.9	−0.07	0.05	−0.06	0.05	−0.08	0.05	−0.07	±	0.05		n.d.				
	2	10.5	−0.09	0.05	−0.05	0.05	−0.10	0.05	−0.06	±	0.05					n.d.	
	3	11.2	−0.03	0.05	−0.06	0.05	−0.05	0.05	−0.06	±	0.05						
Average			−0.06	± 0.09	−0.06	± 0.09	−0.07	± 0.09									
Citric acid 0.01 mM pH 5	1	19.1	−0.10	0.05	−0.15	0.05	−0.10	0.05	−0.14	±	0.05						
	2	16.2	−0.12	0.05	−0.07	0.05	−0.03	0.05	−0.07	±	0.05		n.d.			n.d.	
	3	16.0	−0.07	0.05	−0.01	0.05	−0.09	0.05	−0.03	±	0.05						
Average			−0.10	± 0.09	−0.08	± 0.09	−0.08	± 0.09									
Citric acid 0.1 mM pH 7	1	69.8	−0.29	0.05	−0.11	0.09	−0.29	0.08	−0.13	±	0.05	−0.12	±	0.13	0.17	±	0.14
	2	67.2	−0.31	0.08	−0.14	0.09	−0.29	0.14	−0.16	±	0.07	−0.17	±	0.18	0.15	±	0.20
Average			−0.30	± 0.08	−0.13	± 0.10	−0.29	± 0.12				−0.14	±	0.18	0.16	±	0.20
Oxalic acid 0.01 mM pH 7	1	18.8	−0.06	0.05	−0.09	0.05	−0.12	0.05	−0.09	±	0.05						
	2	19.5	−0.07	0.05	−0.05	0.05	−0.07	0.05	−0.05	±	0.05		n.d.			n.d.	
	3	19.5	−0.08	0.05	−0.04	0.05	−0.08	0.05	−0.05	±	0.05						
Average			−0.07	± 0.09	−0.06	± 0.09	−0.09	± 0.05									
Oxalic acid 0.01 mM pH 5	1	17.6	−0.11	0.05	0.00	0.05	−0.11	0.05	−0.02	±	0.05						
	2	19.3	−0.07	0.05	−0.10	0.05	−0.09	0.05	−0.09	±	0.05		n.d.			n.d.	
	3	16.7	−0.07	0.05	−0.10	0.05	−0.11	0.05	−0.10	±	0.05						
Average			−0.08	± 0.09	−0.07	± 0.09	−0.10	± 0.05									
HA 40 mg/L	1	30.3	−0.14	0.10	−0.02	0.11	−0.07	0.09	−0.03	±	0.09						
	2	30.1	−0.10	0.06	−0.08	0.08	−0.12	0.07	−0.09	±	0.05		n.d.			n.d.	
	3	29.7	−0.11	0.05	−0.03	0.06	−0.10	0.06	−0.05	±	0.05						
Average			−0.12	± 0.12	−0.04	± 0.15	−0.10	± 0.05									
HA 80 mg/L	1	47.9	−0.08	0.10	−0.02	0.14	−0.12	0.05	−0.04	±	0.08						
	2	47.5	−0.12	0.05	−0.10	0.07	−0.13	0.05	−0.10	±	0.05		n.d.			n.d.	
	3	46.9	−0.09	0.05	−0.03	0.13	−0.15	0.20	−0.05	±	0.05						
Average			−0.10	± 0.12	−0.05	± 0.20	−0.13	± 0.07									
HA 110 mg/L	1	55.8	−0.08	0.05	−0.09	0.01	−0.09	0.05	−0.09	±	0.05		n.d.			n.d.	
	2	58.5	−0.10	0.05	−0.20	0.09	−0.10	0.05	−0.15	±	0.05						
Average			−0.08	± 0.06	−0.12	± 0.06	−0.10	± 0.05									

n.d.:not determined.

plexed with organic ligand is between 10% and 20%. In those experiments, the measured $\delta^{60}Ni_A$ and $\delta^{60}Ni_D$ values were not distinguishable from the initial $\delta^{60}Ni$ solution (−0.11 ± 0.05) within analytical uncertainty, neither as a function of pH, nor as a function of the ligand.

According to a study based on Fourier-transformed infrared (FTIR) and X-Ray absorption (XAS) spectroscopies, carboxylic acids with two or more space-close carboxylate functional groups, or with an alcohol donor group adjacent to the carboxylate, form a stronger interaction with Ni, than would do monocarboxylate or polycarboxylate functions separated by methylene groups (Strathmann and Myneni, 2004). Based on FTIR results, Strathmann and Myneni (2004) observed a stronger interaction between Ni and oxalic acid than between Ni and citric acid (Strathmann and Myneni, 2004). The same conclusion was reached by the XAS study reported by Montargès-Pelletier et al. (2008). As bond strength between metal and ligand is thought to influence metal isotopic fractionation (Jouvin et al., 2009; Ryan et al., 2014; Wilcke, 2010), a different $\Delta^{60}Ni_{bond\text{-}free}$ value between Ni-citrate and Ni-oxalate is expected. However, the large predominance of Ni^{2+} in the donor solution in these experimental conditions might have masked the isotopic fractionation and its different entity between the two ligands. It is, therefore, only possible to affirm that no difference between the two ligands can be observed for Ni complexation rates lower or equal to 20% in those settled experimental conditions.

Increasing, indeed, the concentration of citric acid to 0.1 mM, a larger fraction of Ni was complexed, reaching 70%, and the DMT compartment presented distinguishable values in isotopic composition (Fig. 1 and Table 2). However, the calculated values of $\delta^{60}Ni\text{-}L$ and the consequent $\Delta^{60}Ni_{bound\text{-}free}$ results were affected by a considerable incertitude, allowing only affirming that the isotopic fractionation of Ni induced by complexation with citric acid is lower than 0.2‰. As already mentioned above, the low solubility of Ca-oxalate prevented performing similar experiment (high Ligand/Ni ratio) with oxalic acid.

3.3. Alyssum murale *and* Rinorea bengalensis *leaf degradation*

Nickel content and isotopic composition in leaves of *A. murale* and *R. bengalensis* before degradation experiments are reported in Table S3–4. Element concentrations in leaves before leaching experiments and in leaching solutions are reported in Tables S5-8.

Nickel concentrations in leachate solutions of *A. murale* and *R. bengalensis*, and the corresponding Ni isotopic compositions are reported in Fig. 2a–b and Fig. 3a–b, and listed in Tables S3–4.

In the present study, leaching experiments on *A. murale* were conducted in presence and absence of NaN_3. Nickel concentration was measured as a function of time and a mass balance was estimated assuming that [Ni] was constant between two consecutive samplings. Considering the flow rate of 0.5 mL min^{-1} multiplied for the time between two consecutive samplings, it was calculated that after one week the 75%-80% of Ni originally contained in leaves was leached out in absence and in presence of NaN_3, respectively. At the end of the experiment, between 80% and the 90% of Ni was released, in absence and presence of the biocide, respectively. The continuous and the dotted lines in Fig. 2b indicate the average Ni isotopic compositions (triplicate) of *A. murale* leaves before degradation and the corresponding standard deviation, $\delta^{60}Ni_{Alys}$ = 0.19 ± 0.07‰. In addition, this value is close to the one measured by Estrade et al. (2015) on aerial parts of *A. murale* specimen, collected in the same geographical area in Albania (Estrade et al., 2015). During the entire experiment, $\delta^{60}Ni$ value in leachate solutions overlapped, within the incertitude range, the $\delta^{60}Ni$ initially measured for the pristine leaves. No significant difference was observed between experiments conducted in presence and absence of biocide. In these experimental conditions it was not possible, therefore, to estimate the contribution of microbial activity, which was expected to significantly influence both kinetics of metal release and isotopic signature of leachate.

In the case of *R. bengalensis*, leaching experiment was conducted only in presence of NaN_3. Similarly to *A. murale*, > 80% of total Ni was leached out during the first 10 days, and after 30

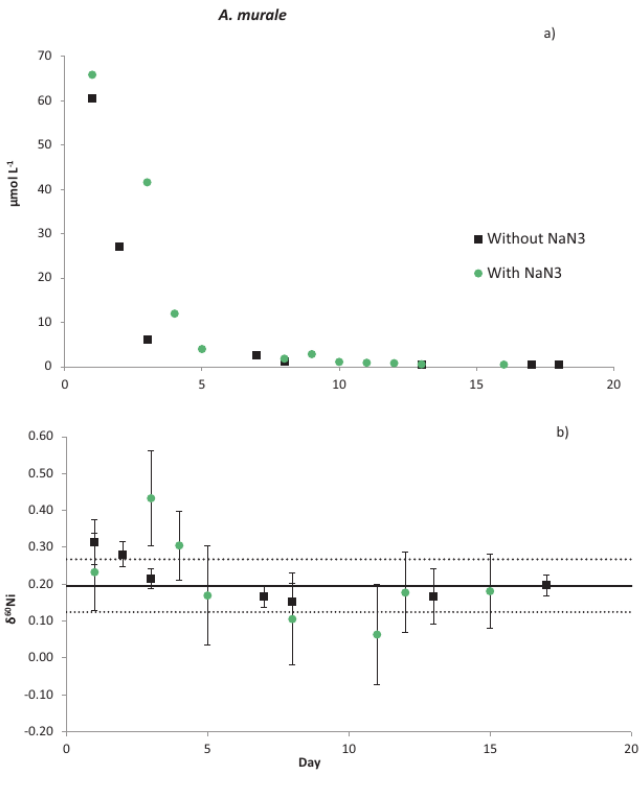

Fig. 2. Alyssum murale *leaf leaching experiments in presence (green points) and absence (black squares) of NaN_3. a) Ni concentration (µmol L^{-1}) in the leached solution as a function of time. b) δ^{60}Ni value in the leached solution. The continuous and dot black lines indicate the average isotopic composition of leaves before leaching and the corresponding standard deviation.*

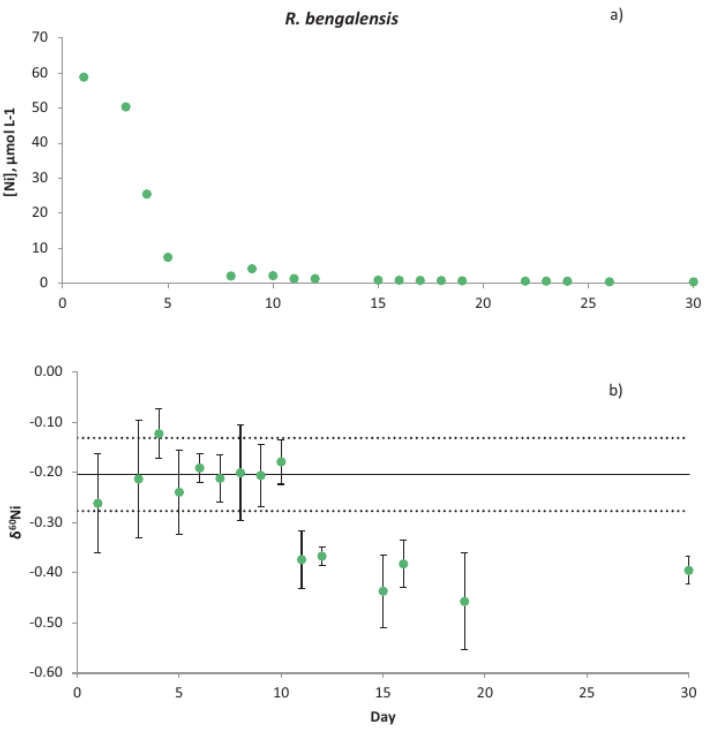

Fig. 3. Rinorea bengalensis *leaf leaching experiments in presence of NaN_3. a) Ni concentration (µmol L^{-1}) in the leached solution as a function of time. b) δ^{60}Ni value in the leached solution. The continuous and dot black lines indicate the average isotopic composition of leaves before leaching and the corresponding standard deviation.*

days of leaching, about 90% of the total Ni was recovered. The average value of $\delta^{60}Ni$ between 1 and 10 days was −0.20 ± 0.05‰, corresponding to $\delta^{60}Ni$ of the original leaves, i.e. -0.19 ± 0.07‰. Interestingly, the solution leached between 10 and 30 days, clearly displayed an enrichment in lighter isotopes, with $\delta^{60}Ni$ = −0.40 ± 0.05‰. The difference between average $\delta^{60}Ni_{10days}$ and $\delta^{60}Ni_{30days}$ was calculated, obtaining $\Delta^{60}Ni_{10-30day}$ = 0.20 ± 0.05‰ and highlighting the presence of at least two pools: the main one, not presenting any fractionation, and a second one providing a release of light isotopes. Unfortunately, it was not possible to check the isotopic signature of Ni remaining in *R. bengalensis* leaves at the very end of those leaching experiments. However, to complete the mass balance, the 10% of Ni missed is expected to provide an isotopic composition enriched in heavy isotopes. During plant material degradation, the isotopic composition of released Ni could potentially present different values compare to Ni originally contained in the plant. Those differences can mainly depend on Ni speciation and localization in different leaf organs, on microbial activity during leaching experiments, and on isotopic fractionation induced by kinetic phenomena. Previous data on hyperaccumulators have reported an enrichment of heavy isotopes in litter, compared to tree leaves, for both Ni (Wang and Wasylenki, 2017) and Zn (Karlsson and Skyllberg, 2007). Nickel localization has been largely investigated in *Alyssum* species and Ni was observed mainly concentrated in epidermal vacuoles and trichomes (McNear et al., 2005; Broadhurst et al., 2004). According to bulk and micro XAS investigations (Montargès-Pelletier et al., 2008; McNear et al., 2010), Ni in A. murale leaves was shown to be mainly stored as Ni-malate complexes. From similar studies using XAS data, Ni in *R. bengalensis*

was mainly present as associated with citrate, forming 1:1 complex, both in plant tissue and in transport fluids. However, differently from *A. murale*, in *R. bengalensis* the highest Ni concentrations have been observed in spongy mesophylls, and in lower and upper epidermis (Van der Ent et al., 2017). To authors'knowledge, there is no evidence of distinct Ni speciation in the different parts of the *R. bengalensis* leaf, which make difficult to link the observed fractionation to a distinct metal speciation. In the case of Zn in hyperaccumulator plants, a distinction has been proposed between Zn in tetrahedral coordination, forming apoplasmic cell wall complexes, and Zn in octahedral coordination, in the symplasm, suggesting a difference in $\delta^{66}Zn$ values depending of Zn coordination and localization. Moreover, it has been suggested that a change in Zn speciation is luckily to take place readily from living to dead leaves, after which Zn was observed to be in tetrahedral form (Aucour et al., 2015). However, this hypothesis cannot be applied in the case of Ni, as the studies of Ni speciation in *A. murale* and *R. bengalensis* leaves evidenced that Ni was remaining in octahedral coordination. Furthermore, for both plants, there is no evidence of Ni in apoplastic space between cells, and Ni is assumed to be mainly stored in vacuoles. Thus in the case of *A. murale* leaching experiments, Ni is expected to be released in a rather homogeneous way, with no disruption due to different speciation and to the release of Ni strongly bound to cell wall. In the case of *R. bengalensis*, experimental results show that about 10% of Ni released from leaves is enriched in lighter isotopes. The reason of the observed Ni fractionation could lie in a distinct Ni speciation, hardly detected by XAS measurements in bulk mode, due to their very low concentration and due to the averaging effect of bulk mode spectroscopic measurements. Although no strong evidence can support the hypothesis of a distinct chemical speciation, for the last 10% Ni released, the observed isotopic fractionation could be correlated to distinct localizations and/or distinct chemical binding to the leaf cells. Then, it can be supposed that two distinct Ni pools are successively released, corresponding to tissues with distinct rate of degradation, and that might probably induce an isotopic fractionation. Beside this first hypothesis, the fractionation can also find an explanation through the formation of metabolic breakdown products during biomass degradation, reacting with simultaneously released Ni^{2+}. Although such a phenomenon was not observed for *A. murale*, a successive degradation of these secondary Ni compounds could be responsible for the different isotopic composition of Ni^{2+} released between 10 and 30 days in the case of *R. bengalensis*. However, to deeply decipher Ni behaviour during degradation, these results should be thoroughly discussed by supplementary data on Ni speciation in leachate solutions and in *R. bengalensis* leaves, at different steps of the leaching experiment.

3.4. Implication for the global Ni biogeochemical cycle

In order to use Ni isotopic signature as a tool to decipher Ni biogeochemical cycle on the Earth's surface layers, it is fundamental to identify and characterize mechanisms and processes that are responsible for Ni isotopic fractionation. Reported results aimed to furnish, for the first time, new data about Ni isotopic fractionation produced during interaction with organic matter and during the degradation of plant biomass.

Our results showed that, for the applied experimental conditions, where only carboxylic groups were involved in Ni complexation, Ni interaction with humic acids did not induce a measurable isotopic fractionation, despite the high affinity of humic acids for metals and their influence on metal mobility. Similarly, for small organic acids, a difference between oxalic and citric was expected on the basis of the stronger bonds formed between Ni and oxalate, but, in the settled experimental conditions, no direct correlation has been found between bond strength and the induced isotopic fractionation. Moreover, only for citric acid $\Delta^{60}Ni_{citrate\text{-}free} < 0.20‰$ was calculated. Recently, a study about Ni distribution and speciation in a malaysian hyperaccumulating plant, *R. bengalensis*, highlighted the predominance of Ni-citrate complexes, both in plant tissues and transport fluids (Van der Ent et al., 2017). Other studies have evidenced Ni in hyperaccumulating plants univocally associated with carboxylic acids, in partic-

ular with citric and malic acids, and only a small fraction presents as free ion (Van der Ent et al., 2017; Lee et al., 1977). However, the fractionation induced by Ni-citrate formation as we demonstrated through DMT experiments is not high enough to justify Δ^{60}Ni values in hyperaccumulators reported in literature. A study about Ni uptake by plants grown in hydroponic conditions (Deng et al., 2014) reported, indeed, the enrichment in Ni light isotopes in all plants compared to starting media, $\Delta^{60}Ni_{plant\text{-}solution}$ = −0.90‰ to −0.21‰. This enrichment was attributed to the Ni low affinity transport system across root cell membranes, coherent with the absence of Ni high-affinity transporters in higher plants (Deng et al., 2014). The effect of Ni concentration gradient in the hydroponic solutions was also combined with kinetic isotopic fractionation, as heavy isotopes move more slowly. In parallel, a translocation of Ni light isotopes from roots to shoots was also observed, $\Delta^{60}Ni_{shoot\text{-}root}$ = −0.47‰. This fractionation was attributed to xylem loading processes. However, up to now, metal transporters involved in xylem loading have not been identified (Clemens et al., 2002). A comparison of non-hyperaccumulator and hyperaccumulator plants reports a range from 0.04 to 0.73‰ between roots and aerial parts, with the latter being enriched in lighter isotopes (Estrade et al., 2015). However, in the same study, three different fractionation trends between roots and aerial parts, in three different species of hyperaccumulating plants were measured, making difficult to ascribe these trends to specific mechanisms. The different $\delta^{60}Ni$ values were associated to the plant stage of growth, combined with storage and translocation mechanisms involving roots, leaves and phloem. Five principal molecular mechanisms can be mentioned describing metal hyperaccumulation within plants: i) mobilization and uptake from soil, ii) compartmentalization and sequestration in roots, iii) transfer to xylem, iv) transport to tissues, and v) storage in leaf cells (Clemens et al., 2002). All these steps are regulated by the presence of chelating molecules and selective transporters, which influence metal accumulation rate and potentially its isotopic composition. Organic acids, e.g. citric, are thought to be likely involved in metal sequestering in cell vacuoles (Callahan et al., 2006). Nickel complexation with citrate or malate (Montargès-Pelletier et al., 2008; McNear et al., 2010; Van der Ent et al., 2017), therefore, could have been advanced as a possible explanation for isotopic fractionation observed in plants. However, results obtained with DMT system demonstrated that the observed fractionation does not take place during storage process. Other phenomena should be considered, such as Ni interaction with other organic molecules (e.g. during transfer processes) presenting different functional groups, probably at cell wall level, as this was evidenced in the case of Zn distribution (Aucour et al., 2015). Isotopic fractionation due to kinetic phenomena should also be taken into account. Results from leaf degradation experiments showed that during leaf decomposition, the most part (e.g. 80% for *R. bengalensis*) of released Ni presented δ^{60}Ni value corresponding to the original leaves. As plants have previously been shown to take up light isotopes from the Ni heavy bioavailable pool, and it has been observed that light isotopes are translocated first from roots to leaves (Deng et al., 2014; Estrade et al., 2015), plant biogeochemical recycling should represent a light isotope input into surface soils, depending on the degree of fractionation between roots and leaves. Even a small fractionation can have a relevant contribution, in particular in ultramafic area, where hyperaccumulators represent a considerable part of the endemic vegetation, and are able to move tremendous amount of Ni, e.g. almost 5 kg per tree of *R. bengalensis* (Van der Ent et al., 2017; Echevarria, 2018). A quantitative estimation of Ni recycling is still poorly constrained, but reported results add further progress for a better comprehension of specific mechanisms regulating Ni cycle within plants.

4. Conclusions

Due to their role in Ni storage in leaf cells, the complexation with organic acids, e.g. citric acid, could have been advanced as a possible explanation for isotopic fractionation observed in plants. Although a difference between oxalic and citric acids was expected, DMT-based experiments did not highlight quantifiable differences between the

two compounds, not allowing a correlation between bond strength and the induced isotopic fractionation. Surprisingly, humic acids, commonly reported as crucial reactants in soils and waters, did not provoke measurable Ni isotopic fractionation. Leaf leaching experiments evidenced, for *R. bengalensis*, a different isotopic composition of released Ni as a function of time, obtaining $\Delta^{60}Ni_{10-30day}$ = 0.20 ± 0.05‰. This fractionation measured for one single leaching cycle, unraveled the influence of hyperaccumulating plants on Ni isotopic signature in surface soils and waters.

Indeed, although the fractionation observed during Ni release involved a minor percentage of the total Ni present in leaves, e.g. 10–20%, this fractionation cumulates to the fractionation occurring during Ni uptake from soil and inside the plant ($\Delta_{roots-leaves}$). Obtained results help to elucidate some of the mechanisms involved in Ni cycle, but further investigations of specific processes, in individual or cumulative modes, are still needed to widen the knowledge of Ni cycle at larger scale.

Acknowledgments. Authors would like to thank Shui-Jiong Wang and an anonymous reviewer for their useful comments. Authors also thank Prof. Jose Paulo Pinheiro and Dr. Elise Rotureau for their help in setting DMT systems. Prof. Jose Paulo Pinheiro is also gratefully acknowledged for supplying PHA. Dr. Antonty Van der Ent is gratefully acknowledged for organising sampling campaign in Sabah rainforest. Dr. Baptiste Laubie and Prof. Aida Bani are acknowledged for supplying *Alyssum murale* leaves. The authors would like to thank Agence Nationale de la Recherche (ANR) project number ANR-14-CE04-0005-03 (AGROMINE) and ANR-10-LABX-21-01 (LABEX21) for funding. This is CRPG contribution N°2567.

Supporting Information. Supplementary data to this article can be found online at https://doi.org/10.1016/j.chemgeo.2018.02.023.

References

Aucour, A.-M., et al., 2015. Dynamics of Zn in an urban wetland soil plant system: coupling isotopic and EXAFS approaches. Geochim. Cosmochim. Acta 160, 55–69.

Bani, A., Echevarria, G., Sulçe, S., Morel, J.L., Mullai, A., 2007. In-situ phytoextraction of Ni by a native population of Alyssum murale on an ultramafic site (Albania). Plant Soil 293, 79–89.

Benedetti, M.F., Milne, C.J., Kinniburgh, D.G., Van Riemsdijk, W.H., Koopal, L.K., 1995. Metal ion binding to humic substances: application of the non-ideal competitive adsorption model. Environ. Sci. Technol. 29, 446–457.

Broadhurst, C.L., et al., 2004. Simultaneous hyperaccumulation of nickel, manganese, and calcium in Alyssum leaf trichomes. Environ. Sci. Technol. 38, 5797–5802.

Callahan, D.L., Baker, A.J.M., Kolev, S.D., Wedd, A.G., 2006. Metal ion ligands in hyperaccumulating plants. JBIC J. Biol. Inorg. Chem. 11, 2–12.

Cameron, V., Vance, D., 2014. Heavy nickel isotope compositions in rivers and the oceans. Geochim. Cosmochim. Acta 128, 195–211.

Cameron, V., Vance, D., Archer, C., House, C.H., 2007. Nickel stable isotopes as biogeochemical tracers. Geochim. Cosmochim. Acta 71, A141.

Cameron, V., Vance, D., Archer, C., House, C.H., 2009. A biomarker based on the stable isotopes of nickel. Proc. Natl. Acad. Sci. U. S. A. 106, 10944–10948.

Cameron, V., House, C.H., Brantley, S.L., 2012. A first analysis of metallome biosignatures of hyperthermophilic archaea. Archaea 2012, 1–12.

Clemens, S., Palmgren, M.G., Krämer, U., 2002. A long way ahead: understanding and engineering plant metal accumulation. Trends Plant Sci. 7, 309–315.

Deng, T.-H.-B., et al., 2014. Nickel and zinc isotope fractionation in hyperaccumulating and nonaccumulating plants. Environ. Sci. Technol. 48, 11926–11933.

Domagal-Goldman, S.D., Kasting, J.F., Johnston, D.T., Farquhar, J., 2008. Organic haze, glaciations and multiple sulfur isotopes in the Mid-Archean Era. Earth Planet. Sci. Lett. 269.

Echevarria, G., 2018. Genesis and Behaviour of Ultramafic Soils and Consequences for Nickel Biogeochemistry. In: Van der Ent, A., Echevarria, G., Baker, A., Morel, J. (Eds.), Agromining: Farming for Metals. Mineral Resource Reviews. Springer, Cham. http://dx.doi.org/10.1007/978-3-319-61899-9_8.

Estrade, N., et al., 2015. Weathering and vegetation controls on nickel isotope fractionation in surface ultramafic environments (Albania). Earth Planet. Sci. Lett. 423, 24–35.

Fraysse, F., Pokrovsky, O.S., Meunier, J.D., 2010. Experimental study of terrestrial plant litter interaction with aqueous solutions. Geochim. Cosmochim. Acta 74, 70–84.

Fujii, T., Moynier, F., Blichert-Toft, J., Albarède, F., 2014. Density functional theory estimation of isotope fractionation of Fe, Ni, Cu, and Zn among species relevant to geochemical and biological environments. Geochim. Cosmochim. Acta 140, 553–576.

Gall, L., et al., 2013. Nickel isotopic compositions of ferromanganese crusts and the constancy of deep ocean inputs and continental weathering effects over the Cenozoic. Earth Planet. Sci. Lett. 375.

Gueguen, B., Rouxel, O., Ponzevera, E., Bekker, A., Fouquet, Y., 2013. Nickel isotope variations in terrestrial silicate rocks and geological reference materials measured by MC-ICP-MS. Geostand. Geoanal. Res. 37, 297–317.

Jones, D.L., 1998. Organic acids in the rhizosphere – a critical review. Plant Soil 205, 25–44.

Jouvin, D., Louvat, P., Juillot, F., Maréchal, C.N., Benedetti, M.F., 2009. Zinc isotopic fractionation: why organic matters. Environ. Sci. Technol. 43, 5747–5754.

Kalis, E.J.J., Weng, Dousma, F., Temminghoff, E.J.M., Van Riemsdijk, W.H., 2006. Measuring free metal ion concentrations in situ in natural waters using the donnan membrane technique. Environ. Sci. Technol. 40, 955–961.

Karlsson, T., Skyllberg, U., 2007. Complexation of zinc in organic SoilsEXAFS evidence for sulfur associations. Environ. Sci. Technol. 41, 119–124.

Kinniburgh, D.G., et al., 1996. Metal ion binding by humic acid: application of the NICA-Donnan model. Environ. Sci. Technol. 30, 1687–1698.

Lee, J., Reeves, R.D., Brooks, R.R., Jaffré, T., 1977. Isolation and identification of a citrato-complex of nickel from nickel-accumulating plants. Phytochemistry 16, 1503–1505.

Marschner, H., Marschner, P., 2012. Marschner's Mineral Nutrition of Higher Plants. Academic Press.

McNear, D.H., et al., 2005. Application of quantitative fluorescence and absorption-edge computed microtomography to image metal compartmentalization in Alyssum murale. Environ. Sci. Technol. 39, 2210–2218.

McNear, D.H., Chaney, R.L., Sparks, D.L., 2010. The hyperaccumulator Alyssum murale uses complexation with nitrogen and oxygen donor ligands for Ni transport and storage. Phytochemistry 71, 188–200.

Milne, C.J., Kinniburgh, D.G., van Riemsdijk, W.H., Tipping, E., 2003. Generic NICA–Donnan model parameters for metal-ion binding by humic substances. Environ. Sci. Technol. 37, 958–971.

Montargès-Pelletier, E., et al., 2008. Identification of nickel chelators in three hyperaccumulating plants: an X-ray spectroscopic study. Phytochemistry 69, 1695–1709.

Pan, Y., et al., 2015. In-situ measurement of free trace metal concentrations in a flooded paddy soil using the Donnan membrane technique. Geoderma 241–242, 59–67.

Pandey, A.K., Pandey, S.D., Misra, V., 2000. Stability constants of metal–humic acid complexes and its role in environmental detoxification. Ecotoxicol. Environ. Saf. 47, 195–200.

Pokrovsky, O.S., Dupré, B., Schott, J., 2005. Fe–Al–organic colloids control of trace elements in peat soil solutions: results of ultrafiltration and dialysis. Aquat. Geochem. 11, 241–278.

Porter, S.J., Selby, D., Cameron, V., 2014. Characterising the nickel isotopic composition of organic-rich marine sediments. Chem. Geol. 387, 12–21.

Ratié, G., et al., 2015a. Nickel isotope fractionation during laterite Ni ore smelting and refining: implications for tracing the sources of Ni in smelter-affected soils. Appl. Geochem. 64, 136–145.

Ratié, G., et al., 2015b. Nickel isotope fractionation during tropical weathering of ultramafic rocks. Chem. Geol. 402, 68–76.

Reeves, R.D., 2003. Tropical hyperaccumulators of metals and their potential for phytoextraction. Plant Soil 249, 57–65.

Ryan, B.M., Kirby, J.K., Degryse, F., Scheiderich, K., Mclaughlin, M.J., 2014. Copper Isotope Fractionation During Equilibration With Natural and Synthetic Ligands. http://dx.doi.org/10.1021/es500764x.

Strathmann, T.J., Myneni, S.C.B., 2004. Speciation of aqueous Ni(II)-carboxylate and Ni(II)-fulvic acid solutions: combined ATR-FTIR and XAFS analysis. Geochim. Cosmochim. Acta 68, 3441–3458.

Temminghoff, E.J.M., Plette, A.C.C., Van Eck, R., Van Riemsdijk, W.H., 2000. Determination of the chemical speciation of trace metals in aqueous systems by the Wageningen Donnan membrane technique. Anal. Chim. Acta 417, 149–157.

Thurman, E.M., 1985. Organic Geochemistry of Natural Waters. Springer Netherlandshttp://dx.doi.org/10.1007/978-94-009-5095-5.

Van der Ent, A., Mulligan, D., 2015. Multi-element concentrations in plant parts and fluids of Malaysian nickel hyperaccumulator plants and some economic and ecological considerations. J. Chem. Ecol. 41 (4), 396–408.

Van der Ent, A., et al., 2015. Agromining: farming for metals in the future? Environ. Sci. Technol. 49, 4773–4780.

Van der Ent, A., et al., 2017. Nickel biopathways in tropical nickel hyperaccumulating trees from Sabah (Malaysia). Sci. Rep. 7, 41861.

Wang, S.-J., Wasylenki, L.E., 2017. Experimental constraints on reconstruction of Archean seawater Ni isotopic composition from banded iron formations. Geochim. Cosmochim. Acta 206, 137–150.

Wasylenki, L.E., Howe, H.D., Spivak-Birndorf, L.J., Bish, D.L., 2015. Ni isotope fractionation during sorption to ferrihydrite: implications for Ni in banded iron formations. Chem. Geol. 400, 56–64.

Weng, L., Temminghoff, E.J.M., Van Riemsdijk, W.H., 2001. Determination of the free ion concentration of trace metals in soil solution using a soil column Donnan membrane technique. Eur. J. Soil Sci. 52, 629–637.

Wiederhold, J.G., 2015. Metal stable isotope signatures as tracers in environmental geochemistry. Environ. Sci. Technol. 49, 2606–2624.

Wilcke, W., 2010. Copper Isotope Fractionation During Complexation With Insolubilized Humic Acid. 44. pp. 5496–5502.

Willaims, R.J.P., Frausto da Silva, J.J.R., 2003. Evolution was chemically constrained. J. Theor. Biol. 220, 323–343.